




Tuning crystal structure of potassium dihydrogen phosphate at ambient conditions

Yufeng Zhang ¹, Huang Huang,¹ Yile Li,¹ Wei Liu ², Jie Jiang,³ Kai Guo,² Ruobing Yi,² Ziqi Fei,¹ Xue-ao Zhang,^{1,4} Rui Mu ^{5,*}, Xing Liu,⁶ Liang Chen,^{2,†} and Haiping Fang⁷

¹College of Physical Science and Technology, Xiamen University, Xiamen 361005, China

²Department of Optical Engineering, Zhejiang Provincial Key Laboratory of Chemical Utilization of Forestry Biomass, Zhejiang A&F University, Hangzhou 311300, China

³Shanghai Institute of Applied Physics, Chinese Academy of Sciences, Shanghai 201800, China

⁴Jiujiang Research Institute of Xiamen University, Jiujiang 332105, China

⁵School of Aerospace Engineering, Xiamen University, Xiamen 361102, China

⁶Shanghai Applied Radiation Institute, Shanghai University, Shanghai 200444, China

⁷Department of Physics, East China University of Science and Technology, Shanghai 200237, China



(Received 20 April 2021; revised 28 June 2021; accepted 21 September 2021; published 15 October 2021)

At ambient conditions, potassium dihydrogen phosphate (KDP) usually exists in tetragonal structure, and only transforms to monoclinic structure at a temperature around 503 K. In this study, stable monoclinic KDP is developed at room temperature using a mixture of graphene oxides and unsaturated KDP solution. Furthermore, a reversible phase transition between monoclinic and tetragonal structure is observed by tuning the distance between graphene oxide layers. The first-principles calculation suggests that the tetragonal structure is more energetically favorable when KDP is sandwiched by two graphitic surfaces with a large interlayer distance, whereas the monoclinic structure is more stable with a small interlayer distance. This is attributed to the interaction between K^+ cations and π electrons in the graphitic surface, which distorts the local structural configurations. The increase of interaction strength with decreasing interlayer distance not only reduces the crystal-liquid interfacial free energy, which promotes the formation of the monoclinic structure in unsaturated solution, but also stimulates transformation of existing tetragonal KDP to monoclinic structure. The observations shed light on the nucleation mechanism for crystal structure that is usually infeasible and unstable at ambient conditions, and provide an avenue to tune crystal structures for a wide range of metal salts.

DOI: [10.1103/PhysRevMaterials.5.103401](https://doi.org/10.1103/PhysRevMaterials.5.103401)

I. INTRODUCTION

The potassium dihydrogen phosphate (KH_2PO_4 or KDP) crystal is widely used as an optoelectronic material in modern optical technology, such as high-power electro-optical applications [1], optical-field polarization manipulations [2], and frequency conversions [3], due to its unique piezoelectric, ferroelectric, and nonlinear optical properties [4]. It is well known that the crystal symmetry of KDP changes from orthorhombic $Fdd2$ to tetragonal $I42d$ at 123 K, and may further change to monoclinic $P2_1/c$ at around 503 K [5,6]. Such structural transition for XH_2PO_4 -type compounds, which consist of hydrogen-bonded tetrahedral anion (PO_4^{3-}) and monovalent cations ($X = Na^+, K^+, Rb^+, Cs^+$), might be accompanied with a significant increase of proton conductivity, which is much desired for electrolytes in proton exchange membrane fuel cells [5]. Even though the exact mechanism of the thermal events at high temperature is under debate [7], it is generally believed that the monoclinic structure is rather difficult to form and is unstable at room temperature [6,8,9]. However, it is reported that the one-dimensional

monoclinic KDP crystal, which shows nanosecond-pulsed second harmonic power generation, can be developed through a nonequilibrium process [3,10]. These findings pose many intriguing challenges to crystallography, e.g., the nucleation mechanism of KDP.

Normally, the nucleation process is governed by two factors, interfacial free energy and volume Gibbs free energy (or chemical potential) between liquid and crystal phases [11]. The interfacial free energy, which acts as an energy barrier preventing the formation of the nuclei, is attributed to the configurational entropy difference between crystal and solution, according to Spaepen's model [12]. This indicates that the local structural similarity between solution and crystal phases determines the interfacial free energy and crystallization behaviors, as exemplified in liquid metals [13].

Recently, it is reported that unconventional stoichiometry crystals (e.g., Na_2Cl , $CaCl$) can be developed under ambient conditions due to cation- π interaction between the cations in solution and the π -conjugated system in the graphitic surface [14,15]. Such strong interaction might not only lead to different stoichiometry, but also alternate the orientation or atomic arrangement of molecules, which would enable a pathway to tune the crystal structure and yield unusual physical properties [15].

*murui@xmu.edu.cn

†liangchen@zafu.edu.cn

Here, we investigated the crystallization behavior of KDP with the assistance of the π -conjugated electrons in the graphitic surface, and observed formation of stable monoclinic KDP at room temperature using unsaturated KDP solution. Furthermore, we observed a reversible phase transition between tetragonal and monoclinic KDP without an elevated temperature (i.e., much smaller than 503 K). Such phenomena are likely due to distortion of local structural configuration induced by the strong cation- π interaction.

II. EXPERIMENT

The graphene oxide (GO) solution, which consists of 45% oxygen content, with a concentration of 5 mg/ml, was purchased from Wuxi Huaxin Testing Technology Co., Ltd., Jiangsu, China. The KDP powder with a purity over 99.5% (purchased from Xiamen Lvyin Reagent and Glass Apparatus Co., Ltd., Fujian, China) and de-ionized water (DI) were used to prepare KDP solutions of concentrations 0.005, 0.01, and 0.05 mol/l, which are far away from the KDP saturation level [8]. The KDP solutions were mixed with the GO solutions in a 1:1 ratio, and centrifuged at a speed of 2000, 4000, 5000, and 7000 revolutions per minute (rpm) for 1 min. Afterward, 1 ml of mixed solutions extracted from the bottom of a centrifuge tube was dried in an oven at 60 °C for 12 h to form KDP/GO membranes for later characterizations. The reference samples (e.g., the pristine GO membranes) were prepared using the same process without addition of KDP powder in the DI water. Note some of the samples prepared by 0.05 mol/l KDP solution and centrifuged at 7000 rpm are marked as “as-prepared.” The other samples prepared at the same conditions were stored at ambient conditions (around $50 \pm 5\%$ humidity) and in a desiccator (less than $15 \pm 5\%$ humidity) for three days, which are labeled as “moistened” and “dry,” respectively. Some of the moistened samples were dehydrated in the oven at 60 °C for 12 h (labeled as “redesiccated”).

The masses of prepared KDP/GO samples and GO membranes, measured using an analytical balance (Mettler Toledo AL104), were used to estimate the amount of KDP in the samples. The morphologies and thicknesses of the samples were characterized using a scanning electron microscope (SEM; Carl Zeiss FE-SEM Sigma HD), while the crystalline structures were probed by x-ray diffraction (XRD) at ambient conditions (Rigaku Ultima IV) with a Cu $K\alpha$ excitation source. The structural properties of the samples were further analyzed based on their Raman spectra, and recorded with a WITec alpha 300RA using the 488 nm line of an Ar⁺ laser.

All the first-principles calculations were performed using the Vienna *Ab initio* simulation package (VASP) [16]. Electron-ion interactions were described by the projector augmented wave (PAW) approach [17]. The generalized gradient approximation (GGA) with the Perdew-Burke-Ernzerhof (PBE) functional were used for the exchange-correlation interactions [18]. The van der Waals interaction was considered using the DFT-D3 method [19]. The cutoff energy of the plane wave was set at 500 eV. The Monkhorst-Pack scheme was used to sample the first Brillouin area [20]. In the process of crystal structure optimization, the energy convergence standard was set to 1×10^{-4} eV.

III. RESULTS AND DISCUSSION

A. Stable monoclinic KDP and reversible phase transition

The XRD patterns of the as-prepared, moistened, and redesiccated KDP/GO samples are shown in Fig. 1(a) over a 2θ diffraction range of 5°–40°. At least six features are observed in the as-prepared sample. By comparing to the XRD features reported in the literature [8,10] and observed in the KDP powder, the strong features around 25.1° and 27.1° have originated from the (444) and (204) plane of monoclinic KDP, respectively, whereas the feature around 24.0° is associated with the (200) plane of tetragonal KDP. Since no significant amount of KDP crystal precipitated on the surface of the KDP/GO samples, as depicted by the SEM images (in the Supplemental Material, Sec. S1 [21]), the observed XRD features are mainly from KDP crystal located between the GO layers. Note that the optical and transmission electron microscopy (TEM) images of the as-prepared samples are shown in the Supplemental Material, Sec. S1 [21], as well. Furthermore, a broad feature (centered on 9.8°) is linked with periodic structure of the GO layers, which is at 9.4° for the pristine GO samples (i.e., without KDP). This suggests that the presence of KDP reduces the interlayer distance of GO, which is likely due to strong interaction between the K⁺ cation in the KDP solution and the π electron in the graphitic surface. A similar phenomenon has been observed in GO membranes soaked in KCl solution [22]. It will be shown in later discussion that the interlayer distance of GO, which closely correlates with the strength of the cation- π interaction, plays a key role in determining the crystal structure of KDP.

After storing the as-prepared samples at ambient conditions for 3 days (i.e., moistened samples), the features associated with the monoclinic structure of KDP almost vanish, but those linked with tetragonal structure are strengthened, while the feature that originated from GO shifts to 9.1°. In contrast, no significant change in XRD features comparing to that of as-prepared samples is observed for the samples stored in a desiccator (i.e., dry samples) for 3 days, as shown in the Supplemental Material, Sec. S2 [21]. This suggests that the monoclinic KDP is stable in dry conditions for at least 3 days, which is much longer than the lifetime of monoclinic KDP prepared by other methods (e.g., about 30 min for monoclinic KDP prepared by using highly supersaturated KDP aqueous [8]). Furthermore, the monoclinic structure of KDP could be dissolved and/or transformed to tetragonal structure after absorbing moisture. Interestingly, such changes in crystal structure are reversible after removing moisture from the samples, as observed in XRD patterns for the redesiccated samples. Note that the GO feature also shifts back to 9.7° for the redesiccated samples. Hence, the phase transition is closely associated with the change in the interlayer distance of GO. As shown in the Supplemental Material, Sec. S3 [21], the reversible phase transition is repeatable even after storing the samples at ambient conditions for 6 months. However, the intensities of the characteristic features in the XRD pattern associated with monoclinic KDP greatly decrease after two cycles (i.e., from monoclinic to tetragonal phase), which is likely due to residual moisture or structural change in GO membranes (e.g., surface adsorbates, passivation).

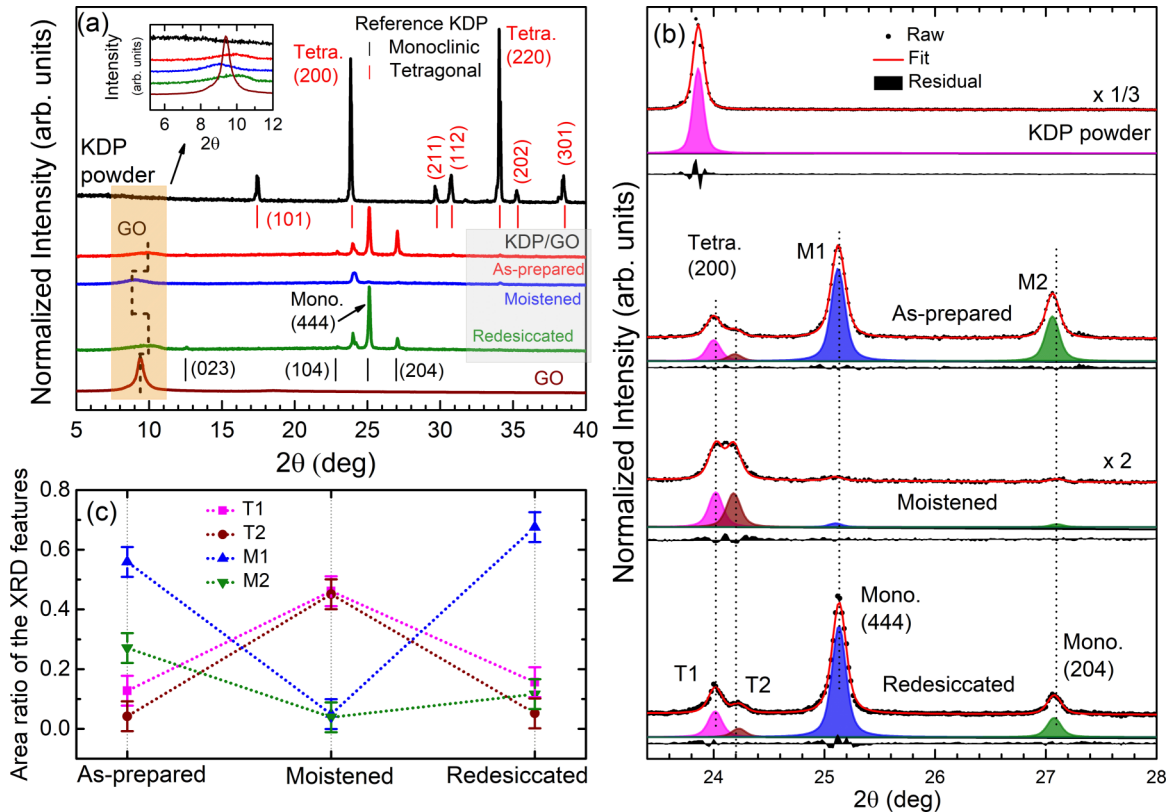


FIG. 1. (a) The XRD patterns of as-prepared, moistened, and redesiccated KDP/GO samples are displaced along with the results of the GO membranes and KDP references. The inset is an enlargement of the region corresponding to the GO feature. Note that the patterns are shifted vertically for easier comparison. (b) The curve fit for the dominant features corresponding to monoclinic and tetragonal structures. (c) The evolution of area ratio of each fit component.

Nevertheless, to quantitatively analyze such changes, a curve fitting analysis was performed for the XRD patterns of the KDP/GO samples and KDP powder over a 2θ diffraction range of 23° – 28° , using a linear background and multiple Voigt functions with equal Gaussian and Lorentzian widths, as shown in Fig. 1(b). At least two Voigt functions (i.e., T1 and T2) are needed to provide a reasonable fit for the feature associated with the (200) plane of tetragonal structure for the KDP/GO samples, while only one Voigt function is enough for that of KDP powder. This suggests that the tetragonal structure with the presence of GO is likely deformed, due to the presence of cation- π interaction. Furthermore, the decreasing interlayer distance of GO (around 0.94 nm) might also limit the relaxation of the H_2PO_4^- clusters during the nucleation process, and leads to a disordered tetragonal structure.

After exposing to moisture and redesiccating, the spectral positions of T1, T2, M1, and M2 do not change much. But the area ratios (i.e., area of the specific component over the total area of all four components) vary dramatically, as shown in Fig. 1(c). Exposing to moisture results in a significant increase of the T1 and T2 intensity ratio, while the M1 and M2 intensities decrease to merely 5%. This could be attributed to two factors: dissolving of monoclinic structure by moisture, and transformation of monoclinic to tetragonal structure. By comparing the masses of the as-prepared and moistened

samples, the absorbed water is only about 0.4 mg, while the mass of KDP in the samples is around 2.8 mg, as shown in the Supplemental Material, Sec. S4 [21]. Absorbing such a small amount of water is not likely to fully dissolve KDP in the samples (i.e., only 0.15 mg KDP based on its solubility at room temperature [23]). Hence, a significant portion of the monoclinic structure is transformed to tetragonal structure. Moreover, the spectral intensities of M1 and M2 increase after desiccating the moistened samples. This suggests that such phase transition is reversible by removing moisture from the samples. Note that the intensity of the M2 feature decreases rather significantly after the redesiccating process. It is reported that the solvent-solute interactions during cluster formation for nucleation and growth can significantly affect the crystal structure [24]. Furthermore, other factors, such as the saturation rate, might also influence the crystal structure [25]. Therefore, recrystallization of KDP in the redesiccating process could lead to a change in KDP crystal orientation and result in a different M2 intensity.

To further investigate the crystal structure of KDP in GO membranes, the KDP/GO samples and references (i.e., KDP powder and GO) are characterized by Raman spectroscopy, as shown in Fig. 2(a). Note that the spectra were normalized to the background. The dominant feature in KDP powder is around 915 cm^{-1} , which corresponds to the tetragonal KDP [26]. Two intense signals were observed at 1356 and

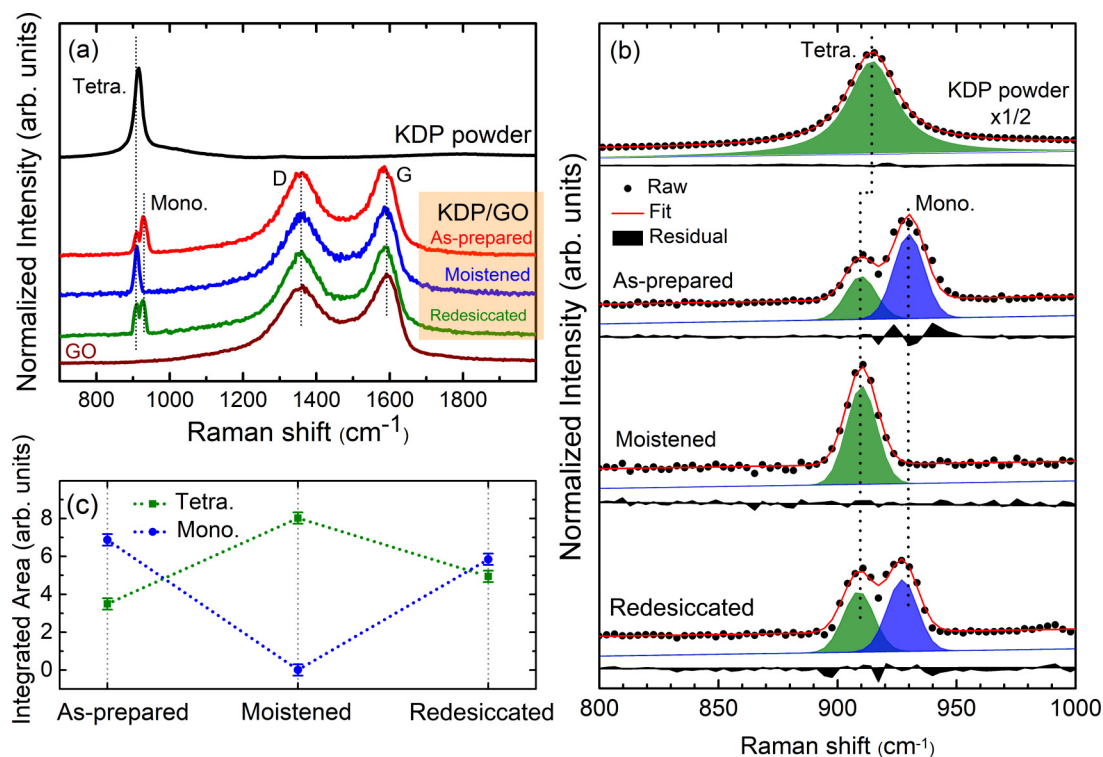


FIG. 2. (a) The Raman spectra of as-prepared, moistened, and redessiccated KDP/GO samples as well as the GO and KDP references. (b) The curve fit for the dominant features corresponding to monoclinic and tetragonal KDP structures. (c) The integrated area of each fit component.

1591 cm^{-1} , which are assigned to the *D* and *G* peaks [27], respectively, for the KDP/GO and GO samples. Furthermore, a feature around 920 cm^{-1} is observed for the KDP/GO samples.

To quantitatively analyze the feature, a curve fit with a linear background and one or two Voigt functions was carried out for the KDP/GO samples and KDP reference, which are shown in Fig. 2(b). At least two Voigt functions are needed for a reasonable fit of the feature for the as-prepared and redessiccated samples, whereas only one Voigt function is sufficient for the KDP powder and moistened samples. By comparing with the literature [8], the components centered at 910 and 930 cm^{-1} are associated with tetragonal and monoclinic KDP, respectively. The spectral intensities of the corresponding features are depicted in Fig. 2(c). The evolution of the tetragonal and monoclinic features is consistent with those observed in XRD patterns.

Generally, the H_2PO_4^- exists in monomers of hydrated clusters in unsaturated KDP solution [28]. Only when the solution is supersaturated would the dimers, trimers, and higher polymers develop and lead to a significant distortion of local configuration of the H_2PO_4^- clusters. The H_2PO_4^- clusters in the monoclinic structure exist with four different forms, and are structurally more chaotic than those in the tetragonal structure [6,8]. Therefore, the tetragonal structure is dominant in precipitation of the unsaturated KDP solution at room temperature. In contrast, a formation of monoclinic KDP usually requires either a highly supersaturated solution [8] or a nonequilibrium process [10], in which the structural configuration might vary greatly in the solution.

It is reported that the hydrated cations (e.g., K^+ , Na^+ , and Li^+) interact with electrons in not only the aromatic rings but also the oxygen functional groups on the GO surface (e.g., epoxy and hydroxyl groups), which form a stable hydrogen-bond network to bind the cations and GO layers [22,29]. In particular, the interaction energy between the hydrated K^+ cations and GO is comparable to the cation's hydration energy, which leads to a significant distortion of the hydrated K^+ structure and results in a narrower interlayer distance of GO than Na^+ and Li^+ [22]. Undoubtedly, such strong interaction not only influences the hydrated K^+ cations, but also the anions (i.e., H_2PO_4^- in this case), which would twist the structural configuration of the H_2PO_4^- clusters. The magnitude of such distortion can be qualitatively linked with the interlayer distance of GO, e.g., smaller interlayer distance indicating a stronger cation- π interaction, more substantial spatial constraint, hence more significant distortion in arrangement of the clusters, as demonstrated by the *ab initio* molecular dynamics simulation reported in the literature [22]. Other tetrahedral anions (e.g., AlCl_4^-) would become distorted/flattened after intercalating into the graphene layers as well [30]. Therefore, it is not surprising to discover monoclinic structure in samples with smaller interlayer distances of GO.

B. Conditions for developing monoclinic KDP

In order to shed light on the correlation between crystal structure of KDP and the distance between the GO layers, the XRD patterns of a set of KDP/GO samples, prepared by 0.05 mol/l KDP solution with different centrifuging speeds

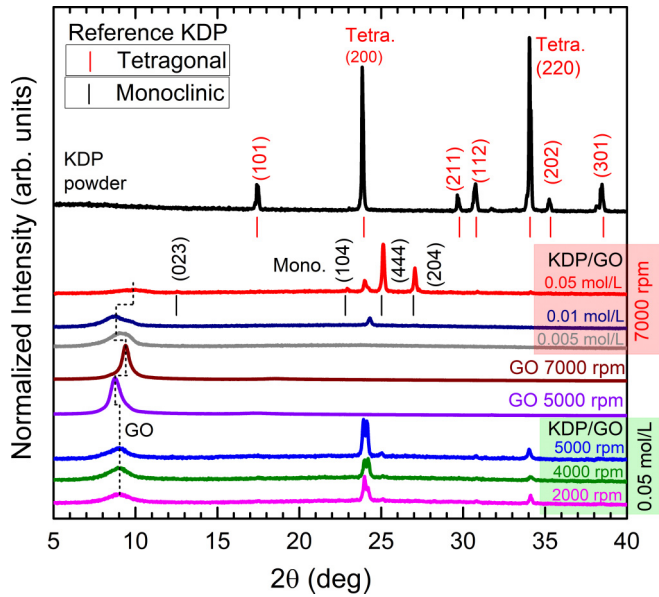


FIG. 3. The XRD patterns of the two sets of KDP/GO samples: (1) prepared by 0.005, 0.01, and 0.05 mol/l KDP solution with a centrifuging speed of 7000 rpm; (2) prepared by a centrifuging speed of 2000, 4000, 5000, and 7000 rpm with 0.05 mol/l KDP solution. The results of GO membranes prepared by a centrifuging speed of 5000 and 700 rpm, as well as KDP references, are shown for comparison.

(i.e., 2000, 4000, 5000, and 7000 rpm), and another set of KDP/GO samples, prepared by various concentrations of KDP solution (i.e., 0.005, 0.01, and 0.05 mol/l) with a centrifuging speed of 7000 rpm, are shown in Fig. 3, as well as those of the reference KDP samples and GO membranes, prepared by a centrifuging speed of 5000 and 7000 rpm. The monoclinic structure is not observed in the KDP/GO samples either prepared with a centrifuging speed that is lower than 7000 rpm or a KDP solution concentration that is smaller than 0.05 mol/l. It is worth noticing that the center of the XRD feature of GO changes from 8.8° to 9.4° , when the centrifuging speed increases from 5000 to 7000 rpm in preparing the GO membranes. This suggests that the interlayer distance of GO prepared in the 7000 rpm centrifuge is smaller ($\sim 10\%$) than that of the 5000 rpm GO membrane. The sedimentation of denser GO sheets in high-speed centrifugation results in a more compact arrangement of the GO sheets (i.e., smaller interlayer distance), which promotes the formation of monoclinic KDP. Note that the other factors might also influence the interlayer spacing of GO, such as oxygen-containing group density [31]. Furthermore, at low KDP concentration (e.g., 0.005 mol/l), the interlayer spacing might increase, which is likely due to intercalation of nanocrystalline KDP in the GO with the absence of strong cation- π interaction.

Even though there is not sufficient water to fully dissolve KDP in the KDP/GO samples, it is still possible to qualitatively explain the reversible phase transition between monoclinic and tetragonal KDP tuned by humidity level, based on nucleation theory for precipitation in solution. After absorbing moisture, the water molecules penetrate the space between the GO layers, and are likely to form hydration with

the K^+ cations, which provides a better Coulomb screening for the cations and reduces the strength of cation- π interaction. This results in an expansion of the interlayer distance, as shown in the inset of Fig. 1(a). Note the centers of the GO features for the KDP/GO samples prepared at a low-speed centrifugation are around 9.0° , which is close to that of the moistened samples (i.e., 9.1°). The increase in interlayer distance would reduce the distortion of the hydrated structure of the K^+ cations as well as the $H_2PO_4^-$ clusters. Therefore, formation of monoclinic KDP is not favored in this circumstance, which leads to a transformation to more ordered structure (i.e., tetragonal structure) and results in an increase of the spectral intensity of T2 in Fig. 1(b). Removing water molecules in the redessicating process leads to a weaker Coulomb screening of K^+ cations; hence it strengthens cation- π interaction and reduces the interlayer distance. This restores the distortion of local structural configuration and results in a phase transition from tetragonal to monoclinic.

At low KDP concentration, the interfacial free energy becomes higher [32], which is not favorable for forming monoclinic structure. Furthermore, the center of the GO feature in XRD patterns is around 8.8° . This suggests that with low KDP concentration, the amount of KDP molecules was not sufficient to provide adequate cation- π interaction with GO to reduce the interlayer distance, which leaves enough space for the $H_2PO_4^-$ clusters to develop an order arrangement before reaching the nucleation stage. Hence, both KDP concentration and centrifuge speed are critical parameters to generate favorable conditions to develop monoclinic KDP.

C. Theoretical modeling

To gain further insight into the impact of interlayer distance on the crystal structure of KDP, we then performed first-principles calculations. Monolayers of monoclinic and tetragonal KDP are constructed by cleaving the two bulk crystals (as shown in the Supplemental Material, Sec. S5 [21]) in the directions perpendicular to the crystal b axis and c axis, respectively. Then the KDP monolayers are sandwiched between two graphene sheets, as shown in Figs. 4(a) and 4(b). The stabilities of these proposed sandwiched structures are examined by calculating the binding energies using the following equation:

$$\Delta E = E_{\text{system}} - E_{\text{KDP}} - E_{\text{graphene}}, \quad (1)$$

where E_{system} , E_{KDP} , and E_{graphene} represent the energies of the proposed sandwiched structures, monolayer KDP, and graphene, respectively. These energies are internal energies at $T = 0$ K obtained directly from the *ab initio* calculations. The distances between two graphene sheets (d_{GG}) are set in the range of 8.5–12.0 Å, for investigating the effect of graphene interlayer distance on the stability and structure of monolayer KDP.

As plotted in Fig. 4(c), in general, both KDP structures/polytypes become less stable (i.e., increase of binding energy) with the decrease of d_{GG} . ΔE of the sandwiched monoclinic KDP decreases slightly, when d_{GG} changes from 12.0 to 10.5 Å (i.e., from about -0.1 eV at 12.0 Å to -0.4 eV at 10.5 Å), while that of the sandwiched tetragonal KDP

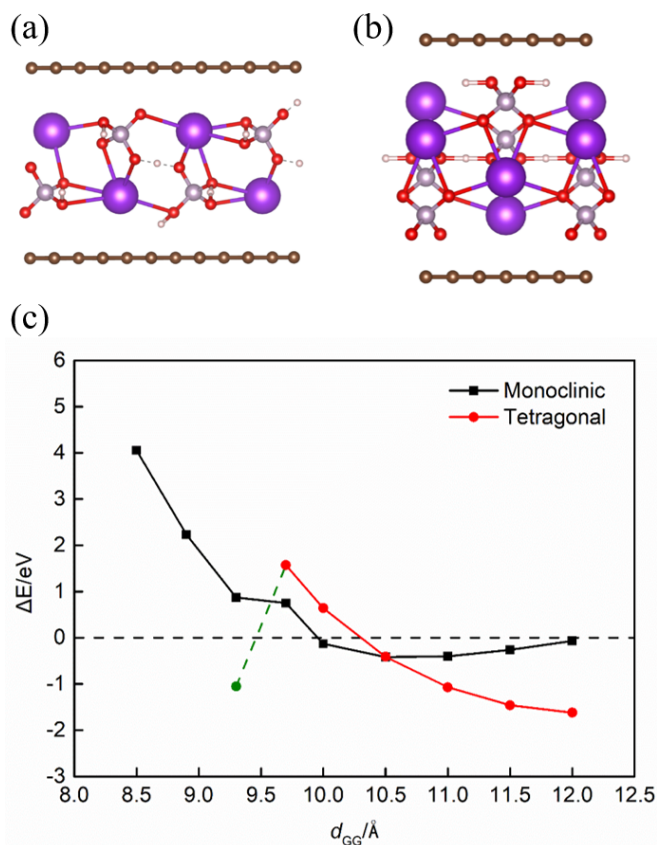


FIG. 4. One layer of (a) monoclinic and (b) tetragonal KDP confined between two graphene sheets. The upper and lower layers of brown spheres represent graphene, while the purple, red, gray, and white spheres represent K, O, P, and H atoms, respectively. (c) Binding energies of monoclinic and tetragonal KDP change as a function of d_{GG} . The black square, red circles, and green circles represent monoclinic KDP, tetragonal KDP, and collapsed structure from tetragonal KDP.

increases significantly (i.e., from about -1.6 eV at 12.0 Å to -0.4 eV at 10.5 Å). The binding energy of the sandwiched tetragonal KDP increases faster than that of the sandwiched monoclinic KDP, with further decrease of d_{GG} (i.e., from 10.5 to 9.5 Å). Hence, the sandwiched tetragonal KDP is more stable than the sandwiched monoclinic KDP, when d_{GG} is larger than 10.5 Å, but less stable when d_{GG} is smaller than 10.5 Å. Interestingly, the ΔE of the sandwiched tetragonal KDP dramatically decreases, when $d_{GG} = 9.3$ Å, which is due to collapsing of the tetragonal structure.

The optimized crystal structures are investigated to understand such change in ΔE . All the structures are obtained through a full optimization by keeping d_{GG} at a certain distance. Some of the results (i.e., $d_{GG} = 12.0, 10.5,$ and 9.3 Å) for two different crystal structures are shown in Fig. 5. Note that a full set of optimized sandwiched structures with different d_{GG} is shown in the Supplemental Material, Sec. S6 [21]. Clearly, the structure of monoclinic KDP, as shown in Figs. 5(a)–5(c), is maintained very well during the compression process (e.g., decreasing of d_{GG} from 12.0 to 9.3 Å), which indicates that monoclinic KDP possesses good flexibility. As shown in the Supplemental Material, Sec. S7 [21], in

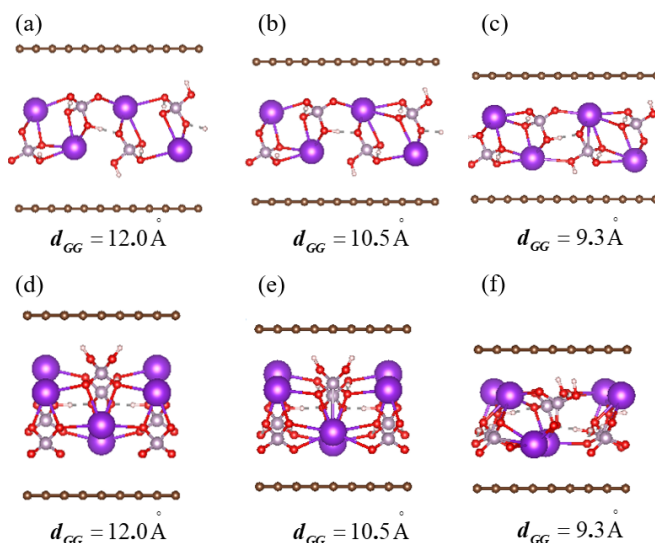


FIG. 5. The optimized structures of sandwiched monolayer KDP with representative values of d_{GG} . (a)–(c) monoclinic KDP and (d)–(f) tetragonal KDP. The upper and lower layers of brown spheres represent graphene, while the purple, red, gray, and white spheres represent K, O, P and H atoms, respectively.

the compression process, the monolayer of monoclinic KDP adapts to the decrease of d_{GG} mainly through the change in bond angles. By contrast, with the decrease of the graphene interlayer distance, the four layers of H_2PO_4^- that are parallel to the graphene planes in the tetragonal structure gradually twist and eventually become two layers, which is similar to the structure of monoclinic KDP, as shown in Figs. 5(d)–5(f). This suggests that the structural deformation of tetragonal KDP is rather large, which is consistent with other reports (e.g., distortion of tetrahedral AlCl_4^- after intercalating into graphene layers [30]). Clearly, when d_{GG} reaches 9.3 Å, KDP molecules are no longer capable of maintaining the tetragonal structure, which results in the significant decrease of ΔE observed in Fig. 4(c). However, KDP is more likely to transform from tetragonal to monoclinic structure with decrease of d_{GG} than maintain tetragonal structure until its collapsing.

The critical interlayer distance derived by the first-principles calculation (i.e., $d_{GG} = 10.5$ Å) is slightly larger than the experimental values (i.e., 9.0 Å for as-prepared samples with monoclinic KDP, and 9.7 Å for moistened samples with tetragonal KDP) derived by XRD. This is likely because the conversion from tetragonal KDP to monoclinic KDP is not a spontaneous process. In other words, at the critical distance, the relative stability of two KDP structures is reversed, but the conversion process will not happen immediately. Nevertheless, the theoretical results confirm that the tendency of structural evolution is closely associated with the change in the interlayer distance of GO, which is in good agreement with the experimental results.

IV. CONCLUSIONS

We develop an approach to form monoclinic KDP at room temperature with unsaturated KDP solution, with the assistance of the interaction between π electrons in the graphitic surface and K^+ cations in KDP. The disordered arrangement

of the hydrated K^+ structure and $H_2PO_4^-$ clusters induced by cation- π interaction provides conditions favorable for the formation of monoclinic structure (i.e., local structural configuration in the solution is closer to that of monoclinic KDP). The monoclinic structure is stable in a dry environment, but can be changed to tetragonal structure by absorbing moisture. Interestingly, the phase transition is reversible by controlling the humidity level in the samples. This is attributed to tuning the magnitude of cation- π interaction by water molecules hydrated with K^+ cations (e.g., Coulomb screening effect) as well as adjusting spatial confinement for the $H_2PO_4^-$ clusters, which results in different levels of distortion in local structural configuration. These observations are of great interest for studying the nucleation mechanism and crystal growth dynamics at ambient conditions. It should be noted that other methods, such as applying strain, can also tune the interlayer distance of GO [31], which offers alternative approaches for controlling the crystal structure, especially for applications where the presence of moisture is not desired. Furthermore, not only K^+ cations in KDP, but also other cations (Na^+ , Li^+ , Fe^{2+} , Co^{2+} , Cu^{2+}) show strong interaction with π -conjugated electrons in the graphitic surface, suggesting the feasibility to apply this method to tune the crystal structures of other metal salts.

ACKNOWLEDGMENTS

The authors thank Professor Guosheng Shi for constructive suggestions. The authors thank Haibo Ke for support with sample preparations and characterizations. This study has been financially supported by the Natural Science Foundation of China (Grants No. 11874423, No. 11975206, No. 12074341, and No. 12174321), and the Fundamental Research Funds for the Central Universities (Grant No. 20720190050).

Y.Z. conceived the idea for the project and analyzed the data. H.H. and Y.L. prepared and characterized materials. W.L., K.G., R.Y., and L.C. designed the theoretical modeling and performed the calculations. J.J. and Z.F. verified the analytical methods. X.L. contributed to the interpretation of the results. X.Z. and H.F. helped supervise the project. R.M. wrote the manuscript and supervised the project. All the authors participated in discussions of the research, and have given approval to the final version of the manuscript.

Y.Z. and H.H. contributed equally to this work.

The authors declare that they have no known competing financial interests or personal relationships that could have appeared to influence the work reported in this paper.

-
- [1] X. Wang, H. Gao, and J. Yuan, Experimental investigation and analytical modelling of the tool influence function of the ultra-precision numerical control polishing method based on the water dissolution principle for KDP crystals, *Precis. Eng.* **65**, 185 (2020).
- [2] H. Ren, Z. Wang, F. Wang, F. Li, X. Sun, and X. Xu, Preparation, characterization and application of ultrathick true zero-order KDP crystal waveplates, *IEEE Access* **7**, 41507 (2019).
- [3] H. Yang, J. Song, D. Li, X. Li, W. Cheng, and Y. Ren, Nanosecond-pulsed frequency-doubled laser in monoclinic single-crystalline KDP microstructures, *IEEE Photon. Technol. Lett.* **31**, 1080 (2019).
- [4] N. Hou, L. Zhang, Y. Zhang, and F. Zhang, On the ultra-precision fabrication of damage-free optical KDP components: Mechanisms and problems, *Crit. Rev. Solid State Mater. Sci.* **44**, 283 (2019).
- [5] C. E. Botez, D. Carbajal, V. A. K. Adiraju, R. J. Tackett, and R. R. Chianelli, Intermediate-temperature polymorphic phase transition in KH_2PO_4 : A synchrotron x-ray diffraction study, *J. Phys. Chem. Solids* **71**, 1576 (2010).
- [6] W. Z. Cai and A. Katrusiak, Structure of the high-pressure phase IV of KH_2PO_4 (KDP), *Dalton Trans.* **42**, 863 (2013).
- [7] I. Piñeres, E. Ortiz, C. De la Hoz, J. C. Tróchez, and C. León, On the nature of the KH_2PO_4 high-temperature transformation, *Ionic* **23**, 1187 (2017).
- [8] S. Lee, H. S. Wi, W. Jo, Y. C. Cho, H. H. Lee, S.-Y. Jeong, Y.-I. Kim, and G. W. Lee, Multiple pathways of crystal nucleation in an extremely supersaturated aqueous potassium dihydrogen phosphate (KDP) solution droplet, *Proc. Natl. Acad. Sci. USA* **113**, 13618 (2016).
- [9] M. Mathew and W. Wong-Ng, Crystal structure of a new monoclinic form of potassium dihydrogen phosphate containing orthophosphacidium ion, $[H_4PO_4]^+$, *J. Solid State Chem.* **114**, 219 (1995).
- [10] Y. Ren, X. Zhao, E. W. Hagley, and L. Deng, Ambient-condition growth of high-pressure phase centrosymmetric crystalline KDP microstructures for optical second harmonic generation, *Sci. Adv.* **2**, e1600404 (2016).
- [11] A. G. Walton, Nucleation of crystals from solution, *Science* **148**, 601 (1965).
- [12] F. Spaepen, A structural model for the solid-liquid interface in monatomic systems, *Acta Metall.* **23**, 729 (1975).
- [13] D.-H. Kang, S. Jeon, H. Yoo, T. Ishikawa, J. T. Okada, P.-F. Paradis, and G. W. Lee, Nanosized nucleus-supercooled liquid interfacial free energy and thermophysical properties of early and late transition liquid metals, *Cryst. Growth Des.* **14**, 1103 (2014).
- [14] G. Shi, L. Chen, Y. Yang, D. Li, Z. Qian, S. Liang, L. Yan, L. H. Li, M. Wu, and H. Fang, Two-dimensional Na-Cl crystals of unconventional stoichiometries on graphene surface from dilute solution at ambient conditions, *Nat. Chem.* **10**, 776 (2018).
- [15] L. Zhang, G. Shi, B. Peng, P. Gao, L. Chen, N. Zhong, L. Mu, L. Zhang, P. Zhang, L. Gou, Y. Zhao, S. Liang, J. Jiang, Z. Zhang, H. Ren, X. Lei, R. Yi, Y. Qiu, Y. Zhang, X. Liu *et al.*, Novel 2D CaCl crystals with metallicity, room-temperature ferromagnetism, heterojunction, piezoelectricity-like property, and monovalent calcium ions, *Natl. Sci. Rev.* **8**, nwaa274 (2020).
- [16] G. Kresse and J. Furthmüller, Efficient iterative schemes for *ab initio* total-energy calculations using a plane-wave basis set, *Phys. Rev. B* **54**, 11169 (1996).
- [17] P. E. Blöchl, Projector augmented-wave method, *Phys. Rev. B* **50**, 17953 (1994).

- [18] J. P. Perdew, K. Burke, and M. Ernzerhof, Generalized Gradient Approximation Made Simple, *Phys. Rev. Lett.* **77**, 3865 (1996).
- [19] S. Grimme, J. Antony, S. Ehrlich, and H. Krieg, A consistent and accurate *ab initio* parametrization of density functional dispersion correction (DFT-D) for the 94 elements H–Pu, *J. Chem. Phys.* **132**, 154104 (2010).
- [20] H. J. Monkhorst and J. D. Pack, Special points for Brillouin-zone integrations, *Phys. Rev. B* **13**, 5188 (1976).
- [21] See Supplemental Material at <http://link.aps.org/supplemental/10.1103/PhysRevMaterials.5.103401> for further details about (Sec. 1) morphologies of the KDP/GO samples; (Sec. 2) the impact of storing environment on the KDP crystal structure; (Sec. 3) the repeatability of the reversible phase transition; (Sec. 4) the masses of KDP/GO samples; (Sec. 5) the crystal structures of monoclinic and tetragonal KDP; (Sec. 6) the fully optimized sandwiched KDP structures with different interlayer distances; and (Sec. 7) the evolution of bond length and bond angle of monoclinic KDP in the compression process.
- [22] L. Chen, G. Shi, J. Shen, B. Peng, B. Zhang, Y. Wang, F. Bian, J. Wang, D. Li, Z. Qian, G. Xu, G. Liu, J. Zeng, L. Zhang, Y. Yang, G. Zhou, M. Wu, W. Jin, J. Li, and H. Fang, Ion sieving in graphene oxide membranes via cationic control of interlayer spacing, *Nature (London)* **550**, 380 (2017).
- [23] P. A. Barata and M. L. Serrano, Thermodynamic representation of the solubility for potassium dihydrogen phosphate (KDP) + water + alcohols systems, *Fluid Phase Equilib.* **141**, 247 (1997).
- [24] W. Li, P. Shi, S. Du, L. Wang, D. Han, L. Zhou, W. Tang, and J. Gong, Revealing the role of anisotropic solvent interaction in crystal habit formation of nifedipine, *J. Cryst. Growth* **552**, 125941 (2020).
- [25] M. Vital, D. Daval, G. Morvan, D. E. Martinez, and M. J. Heap, Barite growth rates as a function of crystallographic orientation, temperature, and solution saturation state, *Cryst. Growth Des.* **20**, 3663 (2020).
- [26] G. Lu, C. Li, W. Wang, Z. Wang, J. Guan, and H. Xia, Lattice vibration modes and thermal conductivity of potassium dihydrogen phosphate crystal studying by Raman spectroscopy, *Mater. Sci. Eng. B* **116**, 47 (2005).
- [27] A. Molla, Y. Li, B. Mandal, S. G. Kang, S. H. Hur, and J. S. Chung, Selective adsorption of organic dyes on graphene oxide: Theoretical and experimental analysis, *Appl. Surf. Sci.* **464**, 170 (2019).
- [28] K. Wojciechowski and W. Kibalczyk, Light scattering study of KH_2PO_4 and BaSO_4 nucleation process, *J. Cryst. Growth* **76**, 379 (1986).
- [29] G. Liu, W. Jin, and N. Xu, Graphene-based membranes, *Chem. Soc. Rev.* **44**, 5016 (2015).
- [30] D. Y. Wang, C. Y. Wei, M. C. Lin, C. J. Pan, H. L. Chou, H. A. Chen, M. Gong, Y. Wu, C. Yuan, M. Angell, Y. J. Hsieh, Y. H. Chen, C. Y. Wen, C. W. Chen, B. J. Hwang, C. C. Chen, and H. Dai, Advanced rechargeable aluminium ion battery with a high-quality natural graphite cathode, *Nat. Commun.* **8**, 14283 (2017).
- [31] Z. Yang, Y. Sun, and F. Ma, Interlayer spacing of multilayer graphene oxide: Influences of oxygen-containing group density, thickness, temperature and strain, *Appl. Surf. Sci.* **529**, 147075 (2020).
- [32] O. Söhnel, Electrolyte crystal-aqueous solution interfacial tensions from crystallization data, *J. Cryst. Growth* **57**, 101 (1982).